Detection and analysis of urban land use changes through multi-temporal impervious surface mapping

GAO Zhihong[1, 2], ZHANG Lu[1], LI Xinyan[3], LIAO Mingsheng[1], QIU Jianzhuang[4]

1. *State Key Laboratory of Information Engineering in Survey, Mapping and Remote Sensing, Wuhan University, Hubei Wuhan* 430079, *China*;
2. *Institute of Remote Sensing Applications, Chinese Academy of Sciences, Beijing* 100101, *China*;
3. *School of Architecture and Urban Planning, Huazhong University of Science and Technology, Hubei Wuhan* 430074, *China*;
4. *School of Information Science and Engineering, Shandong Agricultural University, Shandong Tai'an* 271018, *China*

Abstract: As human activities expanding and the process of urbanization in the past decades, urban land use changes very quickly at different scales in China. Extensive studies have been carried out to extract information of land use changes from remote sensing data. Conventional remote sensing change detection methods such as direct comparison and post-classification comparison are performed at pixel level. However, these methods have been proved to be less effective in quantitatively detecting subtle changes within one land use class than detecting land use transitions, i.e. qualitative changes occurred between different land use classes. To enable the capability of detecting quantitative changes in urban land use, a change detection method is proposed based on impervious surface mapping with multi-resolution remotely sensed data. Urban development leads to the increase of impervious surfaces in urban areas, and the impervious surface has been recognized as an important urban land cover type and one of the key factors in the land, hydrological, climatic, ecological and environmental studies. In this paper, the classification and regression tree (CART) algorithm is used with both high-resolution (QuickBird) and medium-resolution (Landsat5 TM) remote sensing data to establish prediction models of impervious surface percentage (ISP). Based on bi-temporal results of ISP prediction, urban land use changes from 2002 to 2006 are detected in Tai'an city of Shandong province. Furthermore, preliminary analysis for these urban land use changes is carried out. The experimental results demonstrated the feasibility and effectiveness of this change detection method which can be used as a supplement to conventional change detection methods.

Key words: impervious surface, classification and regression tree, land use, change detection

CLC number: TP79/TP751.1 **Document code:** A

Citation format: Gao Z H, Zhang L, Li X Y, Liao M S and Qiu J Z. 2010. Detection and analysis of urban land use changes through multi-temporal impervious surface mapping. *Journal of Remote Sensing.* **14**(3): 593—606

1 INTRODUCTION

Change detection is the process of identifying differences in the state of an object or phenomenon by observing it at different times (Singh, 1989). With the rapid development of urbanization in China, the state and situation of urban land use have changed dramatically, such as the agricultural land around the city has been transformed into urban construction land, the industrial and low-density residential land of the old city have been developed for high-density residential and commercial land. These changes have led to great impacts on the environment and ecological processes gradually. In order to study these impacts, the quantitative change information of land use should be obtained, and the urban land use change detection is very significant (Bruzzone & Serpico, 1997; Mas, 1999; Chen, 2000).

Nowadays, with the rapid development of remote sensing technology, earth observation satellites can provide more and more multi-sensor, multi-temporal and multi-resolution images for land use change detection study (Jia, 2003; Lu *et al*., 2004). The traditional change detection methods include image differencing analysis, the direct classification, post-classification comparison and mixed methods (Coppin *et al*., 2004; Liu *et al*., 2005; Radke *et al*., 2005; Li *et al*., 2005). And most of these methods can obtain pixel-level results using medium-resolution remote sensing images as data source. However, the traditional change detection methods can only extract the transition information of land use types qualitatively rather than quantificationally. In order to solve this problem, Yang *et al*. (2003a) proposed a new urban land use change detection method based on impervious surfaces mapping, and it was applied to the urban expansion monitoring of Atlanta of U.S. successfully.

Impervious surfaces are usually defined as the collection of anthropogenic features through which water cannot infiltrate, typically including buildings, roads, parking lots, sidewalks and

Received: 2009-10-09; **Accepted**: 2009-11-17

Foundation: National Key Basic Research Program of China (No.2007CB714405), Natural Science Foundation of China (No.50808089 and No. 40701122), and the Key Laboratory of Geo-informatics of State Bureau of Surveying and Mapping (No.2009-05).

First author biography: GAO Zhihong (1984—), male, PhD candidate, received the master degree in Cartography and Geographical Information Systems in 2009 from Wuhan University. His research interests include change detection and SAR remote sensing. He has published 6 papers. E-mail: zhgao@irsa.ac.cn

other built surfaces. Impervious surfaces percentage (ISP) is the percentage of impervious surface area in unit surface area. And it has been recognized as a key environmental indicator in studying urban hydrology, heat island effect and thematic mapping (Arnold & Gibbons, 1996; Brabec *et al*., 2002). The number and distribution patterns of impervious surfaces are closely related to urban land use status. The value of ISP corresponding to the same land use type is always in a certain range, and different ISP value represents different land use types. Therefore, the spatial and temporal distribution of ISP can be considered as a continuous description of land use pattern. The method based on ISP can provide more detailed information than traditional land use change detection methods.

Nevertheless, the research and application of the ISP-based change detection method is still in its infancy, and the methods proposed by Yang and other researchers needs further improvements in ISP training/test data collection, optimization of prediction model and analysis of the change detection results. In this study, to achieve the land use change detection method based on ISP, a classification and regression tree (CART) algorithm is used to estimating ISP using multi-source remote sensing data. Tai'an city of Shandong province was chosen as the test area, and the results confirmed the effectiveness of this method.

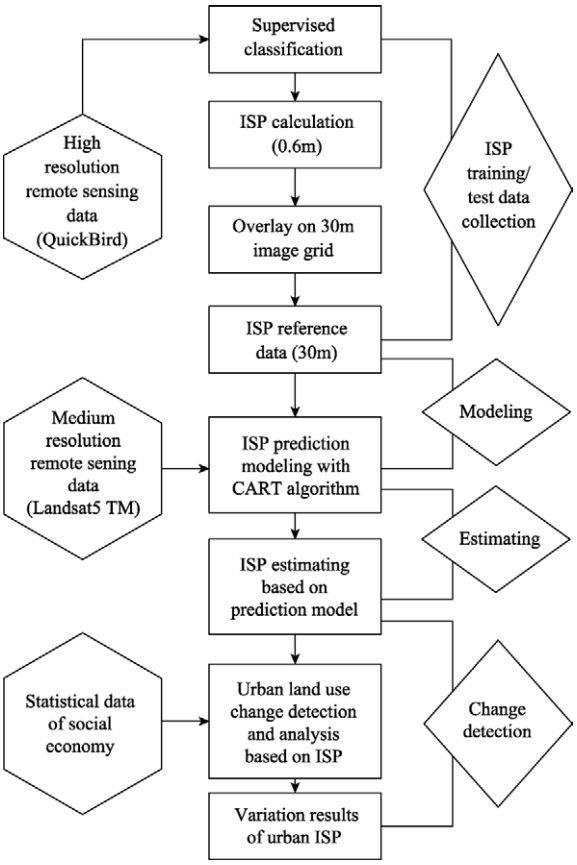

Fig. 1 Flowchart of ISP estimation and urban land use change detection

2 URBAN IMPERVIOUS SURFACE PERCENTAGE ESTIMATING AND LAND USE CHANGE DETECTION

The general process for the ISP-based land use change detection consists of following steps shown in Fig. 1: (1) development of ISP training/test data derived from multi-source remote sensing images; (2) establishment and assessment of final ISP models; (3) ISP estimating, mapping and accuracy assessment; (4) urban land use change detection based on ISP.

2.1 Dataset and pre-processing

Tai'an, located in the middle of Shandong province, is chosen as our study area. Urban area of Tai'an City is located at the southern foot of the world famous Mount Tai. The area exhibits a mixed land-use pattern comprising buildings, transportation, bare land, agriculture, forestry, rivers, reservoir and so on.

Two Landsat5 TM images of Tai'an City acquired in 2002 and 2006 respectively, as shown in Fig. 2, were selected for ISP estimation. Both images were collected in May, which is beneficial for change detection because it can avoid phenological differences. A multi-spectral QuickBird satellite image of May 2005 was used to develop reference data for ISP prediction and performance assessment. All of the images were acquired at

Fig. 2 Landsat5 TM images of Tai'an city (Red: TM4, Green: TM3, Blue: TM2)
(a) May 31, 2002; (b) May 2, 2006

cloud-free condition and had a good quality for experiments. Some basic pre-processing was carried out on the images. The Landsat5 TM and QuickBird images were geometrically corrected to the 1 10000 local terrain map, and re-projected into UTM/WGS84 Projection with pixel size of 30m by 30m for all bands. For relatively clear Landsat5 TM scenes, a reduction in between-scene variability can be achieved through normalization for solar irradiance by converting spectral radiance to planetary reflectance or albedo. The digital value of Landsat5 TM images are transformed into reflectance in this paper (NASA, 2009).

2.2 Methods of ISP estimating and land use change detection

2.2.1 ISP training/test data collection

Successful ISP modeling with the CART algorithm relies on the quality of training/test data. The general process for ISP training/test data collection involves following steps: (1) classification of high resolution images; (2) statistical computation of ISP reference data for ISP modeling and accuracy assessment.

In this research, according to our priori knowledge, supervised classification was used to classify the QuickBird image of 0.6m resolution, and the overall accuracy of 92.56% and kappa coefficient of 0.9112 were achieved. There are nine classes in the classification results including farmland, grassland, forest, bare land, building, road, cement, water and shadow. Classes of building, road, cement were considered as impervious surfaces. Pixels classified as impervious surfaces were then aggregated to estimate ISP over 50×50 grids. The final statistical results were resampled into 30m grids to match the resolution of Landsat5 TM images. Fig. 3 presents a subset of the QuickBird image and corresponding ISP results at 30m resolution. The spatial patterns of the ISP results illustrated in Fig. 3 were generally reasonable; ISP values of the building area are always higher than the vegetation coverage area. Training and test data were derived from a wide range excluding shadow areas. 8000 training samples and 2000 testing samples were independently selected based on stratified random sampling for establishment and evaluation of the rule-based ISP prediction model.

It should be noted that the shadow class was excluded from the ISP calculation due to its uncertain status. In addition, if the high-resolution and medium-resolution images are acquired in different years, the samples which do not have the same type of ground features should be discarded in order to avoid possible degradation in performance of ISP prediction models.

2.2.2 ISP modeling and mapping

In order to build the ISP prediction model, the training data was obtained from the QuickBird image as the target variable (ISP), and the six spectral bands of Landsat5 TM image excluding the thermal infrared band as predictor variables. The final regression tree model was built using the most relevant input variables and all available training data, and then applied to all pixels to map large area. Each classification and regression tree can be represented as a series of decision rules as follows:

Model:

Rule 1: [2165 cases, mean 44.8, range 1 to 99, est err 15.9]

if

band03≤59

band04 > 75

then

dep = –105.6 + 1.85 band03 + 1.5 band02 –0.72 band04 + 0.44 band06 –0.43 band12 + 0.65 band08 + 0.06 band09 + 0.03 band11

Rule 2: [1498 cases, mean 63.8, range 1 to 100, est err 13.4]

if

band03≤59

band04≤75

then

dep = –63.9 + 3.1 band03 –1.45 band04 + 0.8 band09 + 1.02 band02 + 0.3 band05 –0.53 band07 –0.33 band06 + 0.22 band11 –0.04 band12

Rule 3: [1527 cases, mean 71.9, range 1 to 100, est err 14.9]

if

band03 > 59

band04 > 77

then

dep = 57.3 + 2.09 band02 –1.12 band03 –1.02 band04 + 0.56 band01 –0.22 band05 + 0.43 band09 + 0.27 band06 –0.35 band07 + 0.22 band10

Rule…

Each rule set defined the conditions under which a multivariate linear regression model was established and can account for a nonlinear relationship between predictive and target variables. The initial predictive models were developed based on CART algorithm by using the Cubist 2.05 software in this paper.

2.2.3 Accuracy assessment of ISP estimating

The final ISP estimating results were obtained by applying the ISP prediction models of 2002 and 2006 respectively. In order to speed up the computation, open water areas were masked before ISP estimation. To ensure the validity of the assessment, all the reference data were selected randomly and independently from the training data used in building the ISP prediction models. Besides the average error (AE) and relative error (RE), correlation coefficient (r) between actual and predicted values was also used to evaluate the quality of ISP prediction models. All three statistical measures were used throughout the study to evaluate the ISP model performance (Yang *et al*., 2003a, 2003b; Wu & Murray, 2003; Xian & Crane, 2005).

2.2.4 Urban land use change detection based on ISP

A pair of urban ISP estimating results was obtained using the Landsat5 TM images of 2002 and 2006. Land use change detection and analysis of Tai'an City was conducted base on the variation map obtained by ISP image differencing.

3 RESULTS AND ANALYSIS

3.1 Results of ISP estimating and accuracy assessment

The ISP maps of 2002 and 2006 obtained are shown in Fig. 4, in which different colors represent different ranges of ISP value. It can be seen that spatial patterns of the two estimation results are generally similar to each other. The models correctly predicted the high ISP values as more than 60% in dense built-up areas, and even higher (80%—100%) in the old city. However, the ISP at suburbs and hilly areas located in the south and north of the study area are lower than 40% obviously. The ISP value is lower than 30% in most vegetated areas, and is always between 40% and 50% in the bare land area. The experiment results indicated that the ISP prediction models quantified the general impervious surface of the study area reasonably.

An accuracy assessment was performed to evaluate the ISP estimation results using the 2000 independent samples, and the results are shown in Table 1. Fig. 5 shows the scatter plots of correlation coefficient r which presents the agreement between the actual values of the target attribute and those values predicted by models. Table 1 shows that the performances of the two ISP prediction models are comparable, the prediction model

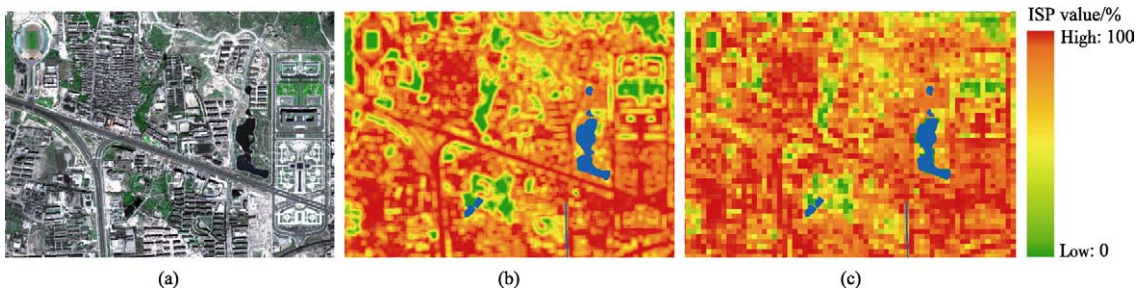

Fig. 3 Extraction of training/test data for ISP estimation
(a) pan-sharpened QuickBird image of 0.6m resolution; (b) ISP map of 0.6m resolution; (c) ISP map of 30m resolution. Blue color in (b) and (c) indicates waterbody mask

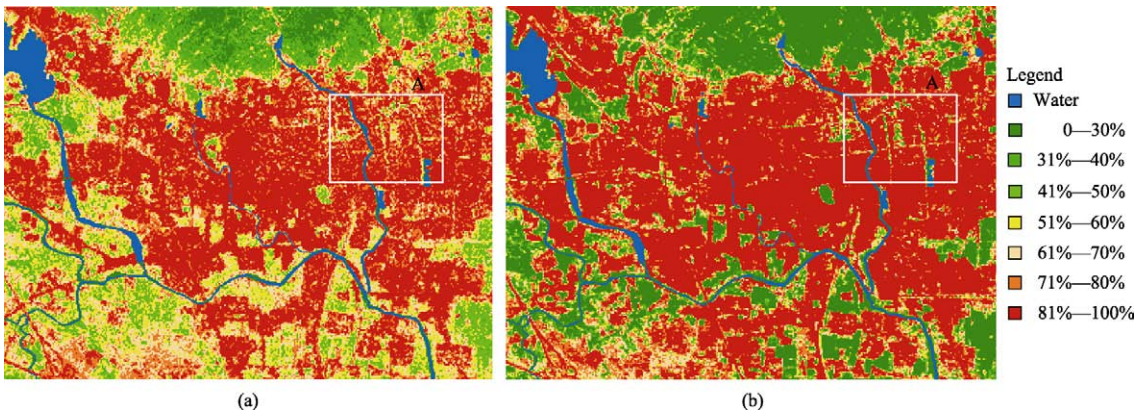

Fig. 4 Results of ISP estimation over Tai'an city
(a) 2002; (b) 2006

of 2006 has a better performance owing to its proximities in acquisition time with QuickBird image. Compared with the prediction model of 2002, the correlation coefficient of 2006 increased by 0.04 and the average error decreased by 1.8%. Generally speaking, the estimation results of Landsat5 TM images are satisfactory, and the predication models have a trend of ISP overestimation for the pixels with low imperviousness (0—20%), but underestimation for those with high imperviousness (80%—100%).

3.2 Results and analysis of change detection

The ISP variation map was obtained by differencing the two results of 2002 and 2006. Fig. 6 shows the distribution of areas with ISP increment. It can be concluded that not only the extent but also the destiny of Tai'an City have changed obviously from 2002 to 2006. The extent of the old city has expanded to the whole test area, and most of the areas with ISP increment exceeding 40% were located in the new built-up areas. Moreover, density of the urban area increased greatly, especially in the old city. For example, the ISP in old city (such as A in Fig. 4) increased from 61%—70% to 81%—100%.

For the purpose of quantitative and qualitative analysis, ISP variation of increasing more than 30% (yellow) and decreasing more than 40% (green) were identified in Fig. 7. Combined with the images and terrain map of Tai'an, it can be found that the areas marked as A, B, C are the areas around the new government building, the Dahe Reservoir dam and the development zone of Tai'an. ISP in these areas increased obviously (more than 30%) caused by constructions from 2002 to 2006. Meanwhile, to improve the tourist environment of Tai'an, a lot of greenbelt was built during the national "tenth five-year", as a result the ISP reduced dramatically in the areas around the foot of the Mount Tai (such as D in Fig. 7) and the development zone of Tai'an (such as E in Fig. 7). NDVI of the two temporal Landsat5 TM images were calculated, and it can be found that NDVI in the areas colored in green (such as D and E in Fig. 7) increased greatly. In other words, the main reason of ISP decrement is the increment of the vegetation coverage. In short, ISP variations can represent the pattern of urban land use change directly.

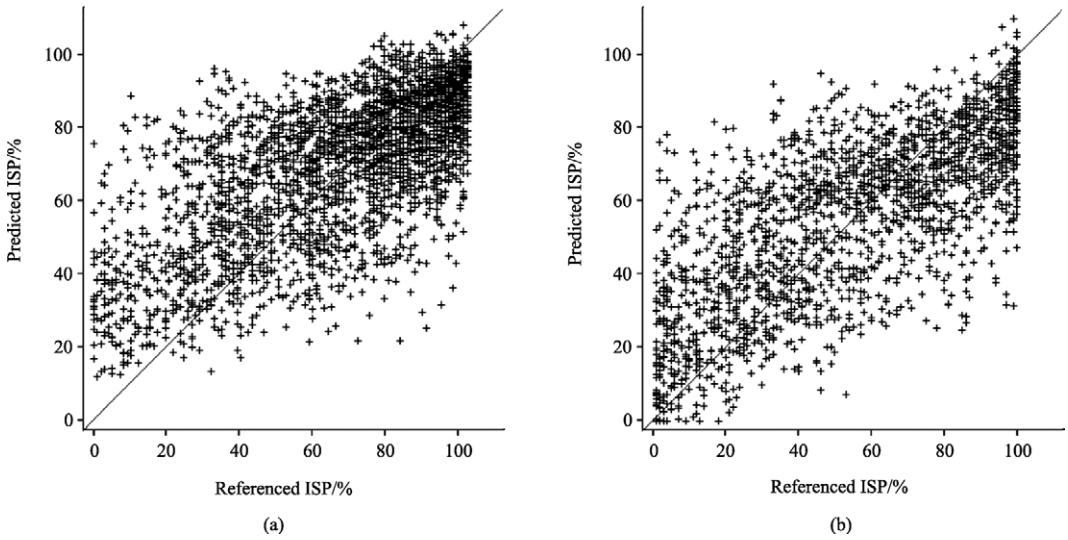

Fig. 5 Scatter plots between predicted and reference ISP in Tai'an
(a) 2002; (b) 2006

Table 1 Accuracy assessment for the two ISP prediction models of Tai'an

Time	Statistical indicators		
	Average error (AE) /%	Relative error (RE)	Correlation coefficient (*r*)
2002	16.9	0.69	0.67
2006	15.1	0.64	0.71

In order to quantitatively analyze the trend in land use changes, urban land use types were divided into four broad categories by ISP values. The empirical thresholds and the dominant components of the four categories are shown in Table 2. Variation of the four categories of land use between 2002 and 2006 were obtained by statistical analysis, shown in Table 3.

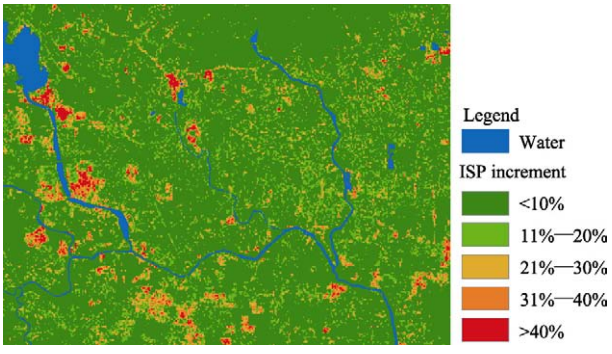

Fig. 6 Results of ISP change detection in Tai'an city from 2002 to 2006 (increase in ISP)

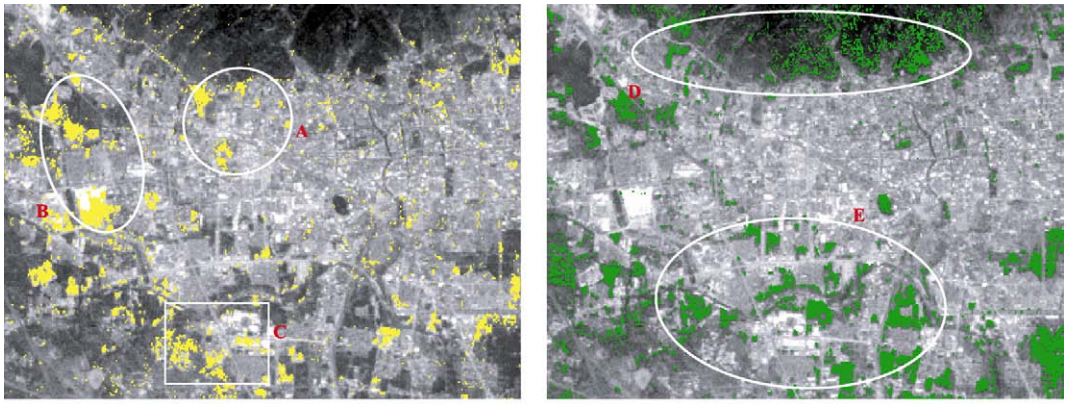

Fig. 7 ISP change maps from 2002 to 2006

(a) Areas with ISP increased by more than 30%, A is the area around the new government building, B is the area below the Dahe Reservoir dam, and C is the development zone of Tai'an; (b) Areas with ISP decreased by more than 40%, D is the area along the foot of the Mount Tai, and E is the development zone of Tai'an and the farmland around it

Table 2 Four urban land use categories according to ISP value

Categories of land use	Non-construction land	Moderate and low density urban land area	Moderate and high density urban land area	High density urban land area
Extent of ISP /%	<30	31—50	51—80	81—100
Dominating feature components	Agricultural land and urban green space	Residential land and a spot of roads	Roads and commercial land	Commercial land and industrial storage sites

Table 3 Variations in area of four urban land use categories in Tai'an from 2002 to 2006

/km^2

Types of land use	2002	2006	Variation
Non-construction land	5.4774	17.7111	12.2337
Moderate and low density urban land area	11.7900	7.2720	–4.5180
Moderate and high density urban land area	36.1089	17.4969	–18.6120
High density urban land area	35.1531	46.0494	10.8963
Total area	88.5294		0

According to above results, characteristics of land use change in Tai'an from 2002 to 2006 were obtained as following:

(1) The transitions between urban land use categories were very obvious, and the density of urban land use increased significantly. The trend discovered was that the moderate and low density urban land area transformed into high density urban land gradually. From 2002 to 2006, the moderate and low density urban land area reduced significantly, while high density urban land area increased by about 10.8963km^2.

(2) The achievements of urban landscape construction were remarkable, the non-construction land of which ISP value were less than 30% increased substantially. From 2002 to 2006, the non-construction land in the experimental area increased from 5.4774km^2 to 17.7111km^2, and the increment was about 223%. Most of the increased non-construction land was urban green space.

4 CONCLUSION AND DISCUSSION

The method of urban change detection based on ISP estimation is investigated in this paper, Tai'an City was chosen as the test area, and the results validated the potential of this method. Compared with traditional methods, the method employed in this paper combines the merits of multi-source remotely sensed data, and it provided a different way to extract and analyze information of the urban land use change by quantifying ISP as an urban indicator. Therefore it can be used as a supplement to conventional change detection methods.

However, there are also some defects of the method used in this paper. Owing to the fact that errors between 10% to 20% exist in the two temporal results of ISP estimation, subtle variations of ISP is difficult to reflect the actual changes of ground features effectively. Moreover, accuracy of the change detection is influenced by the following factors: registration and calibration errors of the multi-source and multi-temporal images, error and uncertainty in the ISP training samples, i.e. processing of the shadow areas in the images and the consistency of the training samples in medium and high images. Nevertheless, with the improvement of remote sensing in image registration, calibration and interpretation, these limitations are expected to be mitigated.

REFERENCES

Arnold C L and Gibbons C J. 1996. Impervious surface coverage: the

emergence of a key urban environmental indicator. *Journal of the American Planning Association*, **62**(2): 243—258

Brabec E, Schulte S and Richards P L. 2002. Impervious surfaces and water quality: a review of current literature and its implications for watershed planning. *Journal of Planning Literature*, **16**(4): 499—514

Bruzzone L and Serpico S B. 1997. An iterative technique for the detection of land-cover transitions in multitemporal remote- sensing images. *IEEE Transactions on Geoscience and Remote Sensing*, **35**(4): 858—867

Chen S P. 2000. Urbanization and Urban Geographical Information System. Beijing: Science Press

Coppin P, Jonckheere I, Nackaerts K, Muys B and Lambin E. 2004. Digital change detection methods in ecosystem monitoring: a review. *International Journal of Remote Sensing*, **25**(9): 1565—1596

Jia Y H. 2003. Digital Image Processing. Wuhan: Wuhan University Press

Li Q, Li L and Zhao X. 2005. Urban change detection using landsat TM imagery. *Geomatics and Information Science of Wuhan University*, **30**(4): 351—354

Liu Z, Gong P and Shi P J. 2005. Study on change detection automatically based on similarity calibration. *Journal of Remote Sensing*, **9**(5): 537—543

Lu D, Mausel P, Brondízio E and Moran E. 2004. Change detection techniques. *International Journal of Remote Sensing*, **25**(12): 2365—2407

Mas J F. 1999. Monitoring land-cover changes: a comparison of change detection techniques. *International Journal of Remote Sensing*, **20**(1): 139—152

NASA. 2009. Chapter 11 - Data product. Landsat 7 science data users handbook. http://landsathandbook.gsfc.nasa.gov/handbook/ handbook_htmls/chapter11/chapter11.html#section11.3[2007-07-12]

Radke R J, Andra S, Al-Kofahi O and Roysam B. 2005. Image change detection algorithms: a systematic survey. *IEEE Transactions on Image Processing*, **14**(3): 294—307

Singh A. 1989. Digital change detection techniques using remotely-sensed data. *International Journal of Remote Sensing*, **10**(6): 989—1003

Wu C and Murray A T. 2003. Estimating impervious surface distribution by spectral mixture analysis. *Remote Sensing of Environment*, **84**(4): 493—505

Xian G and Crane M. 2005. Assessments of urban growth in the Tampa Bay watershed using remote sensing data. *Remote Sensing of Environment*, **97**(2): 203—215

Yang L M, Huang C Q, Homer C G, Wylie B K and Coan M J. 2003. An approach for mapping large-area impervious surfaces-synergistic use of Landsat-7 ETM+ and high spatial resolution imagery. *Canadian Journal of Remote Sensing*, **29**(2): 230—240

Yang L M, Xian G, Klaver J M and Deal B. 2003. Urban land-cover change detection through sub-pixel imperviousness mapping using remotely sensed data. *Photogrammetric Engineering and Remote Sensing*, **69**(9): 1003—1010

城市土地利用变化的不透水面覆盖度检测方法

高志宏[1,2], 张 路[1], 李新延[3], 廖明生[1], 邱建壮[4]

1. 武汉大学 测绘遥感信息工程国家重点实验室, 湖北 武汉 430079;
2. 中国科学院 遥感应用研究所, 北京 100101;
3. 华中科技大学 建筑与城市规划学院, 湖北 武汉 430074;
4. 山东农业大学 信息科学与工程学院, 山东 泰安 271018

摘 要: 通过分析城市中不透水面数量和分布的变化与城市土地利用变化之间的对应关系, 综合中、高分辨率遥感数据各自的优势, 运用CART算法进行城市不透水面覆盖度(ISP)遥感估算, 基于ISP制图结果对城市土地利用变化进行检测。以山东省泰安市为例开展实验研究, 结果表明, 与传统的变化检测方法相比, 基于ISP的变化检测方法, 不仅能够反映土地利用类型转换的潜在信息, 而且可以灵活地量化定义和解释城市用地变化情况。这种方法为城市土地利用变化信息的提取和分析提供了一种新的思路, 可以作为现有变化检测方法的有益补充。

关键词: 不透水面, 分类回归树, 土地利用, 变化检测

中图分类号: TP79/TP751.1 文献标识码: A

引用格式: 高志宏, 张 路, 李新延, 廖明生, 邱建壮. 2010. 城市土地利用变化的不透水面覆盖度检测方法. 遥感学报, **14**(3): 593—606

Gao Z H, Zhang L, Li X Y, Liao M S and Qiu J Z. 2010. Detection and analysis of urban land use changes through multi-temporal impervious surface mapping. *Journal of Remote Sensing*. **14**(3): 593—606

1 引 言

变化检测是一种重要的遥感应用技术, 它是通过对比分析在不同时相观测同一目标对象获取的多幅遥感影像来确定其在状态上的变化和差异(Singh, 1989)。随着近年来中国城市化进程的发展, 城市的土地利用状态和格局发生了剧烈的变化, 包括城市周边的农业用地被征用转变为城市建设用地, 城市老城区的工业用地和低密度居住用地被开发为高密度居住用地和商业用地等, 这些变化对人类生存环境和生态过程的影响已日益凸显。研究这些影响需要定量化地获取城市土地利用变化信息, 因此城市土地利用变化检测的必要性越来越凸显出来(Bruzzone & Serpico, 1997; Mas, 1999; 陈述彭, 2000)。

随着遥感技术的迅猛发展, 对地观测卫星可以提供越来越多的覆盖同一地区的多传感器、多时相和多空间分辨率的影像, 为利用遥感数据进行土地利用变化检测研究提供了丰富的数据源(贾永红, 2003; Lu 等, 2004)。传统的变化检测方法主要包括差异影像分析法、直接分类法、分类后比较法和混合法等(Coppin 等, 2004; 刘臻等, 2005; Radke 等, 2005; 李全等, 2005), 这些方法大多以中分辨率遥感影像作为数据源, 实现的主要是像素级变化检测。对于城市土地利用变化, 采用传统变化检测方法往往只能提取出发生在不同土地利用类型之间的质变, 难以探测到发生在同一土地利用类型内部的量变。为了解决这一难题, Yang 等(2003a)率先提出了基于不透水面制图的城市土地利用变化检测方法, 并成功地应用于美国亚特兰大市的城市扩展遥感监测(Yang 等, 2003a)。

不透水面是一种降水不能直接通过也不能下渗到土壤中的人工地貌特征, 包括城市中的建筑物屋顶、沥青或水泥覆盖的道路、停车场等。不透水面覆盖度(impervious surfaces percentage, ISP)是指单

收稿日期: 2009-10-09; 修订日期: 2009-11-17

基金项目: 国家重点基础研究发展计划(编号: 2007CB714405), 国家自然科学基金项目资助(编号: 50808089, 编号: 40701122)和对地观测技术国家测绘局重点实验室经费资助项目(编号: 2009-05)。

第一作者简介: 高志宏(1984—), 男, 山西忻州人, 武汉大学地图学与地理信息系统专业硕士毕业, 现为中国科学院遥感应用研究所博士研究生。主要从事遥感变化检测, 雷达遥感等方面的研究, 已发表论文 6 篇。E-mail: zhgao@irsa.ac.cn。

位地表面积中不透水面的面积所占的百分比。作为城市环境问题研究中的关键因子，广泛地应用于城市水文过程模拟、热岛效应分析以及城市专题制图等研究中(Arnold & Gibbons, 1996; Brabec 等, 2002)。城市中不透水面的数量和分布格局与城市土地利用形态具有密切的相关性，同一土地利用类型对应的 ISP 在某一连续分布范围内取值，不同土地利用类型对应的 ISP 分布范围一般不同。因此, ISP 的时空分布可视作为对城市土地利用格局的一种连续化描述。基于 ISP 的土地利用变化检测方法应用于城市扩展监测分析，能够提供比传统变化检测方法更多的细节信息，有效地弥补传统方法的局限和不足。

不过，目前基于 ISP 的变化检测方法在中国的研究应用尚处于起步阶段，Yang 等提出的方法在训练和测试数据的选取与处理、预测模型的优化和变化检测结果的分析等方面有待改进和深入的实验研究。本文研究运用分类回归树(classification and regression tree, CART)方法，综合利用中、高分辨率遥感数据，实现了基于 ISP 的城市土地利用变化检测方法，并以山东省泰安市为例开展了实验研究，结果证实了本文方法的有效性。

2 ISP 遥感估算与城市土地利用变化检测

基于 ISP 的土地利用变化检测方法主要包括如下步骤: (1)从中、高分辨率遥感影像获取 ISP 估算的训练数据和测试数据; (2)运用 CART 算法建立 ISP 预测模型; (3)对中分辨率遥感影像应用 ISP 预测模型，进行 ISP 估算和精度评价; (4)比较不同时相的 ISP 估算结果，进行变化检测。具体技术流程如图 1。

2.1 实验数据准备与预处理

选择泰安市作为实验区，泰安地处山东省中部，位于东经 116°50′22″—117°28′44″，北纬 35°52′28″—36°28′33″。泰安市城区坐落于举世闻名的泰山南麓，属于鲁中南低山丘陵区。实验区内主要地物类型有建筑物、道路、空地、林地、农田、河流和水库等，整个实验区内各种地物类型交错分布，地块较为细碎。

选取如图 2 所示 2002 年和 2006 年两景泰安城区的 Landsat5 TM 影像进行 ISP 估算，获取时间均为当年 5 月，这样可以尽量避免季节性物候差异对变化检测的不利影响。由于缺乏同期的地面调查数据，选取了实验区 2005 年 5 月的 QuickBird 影像作为地

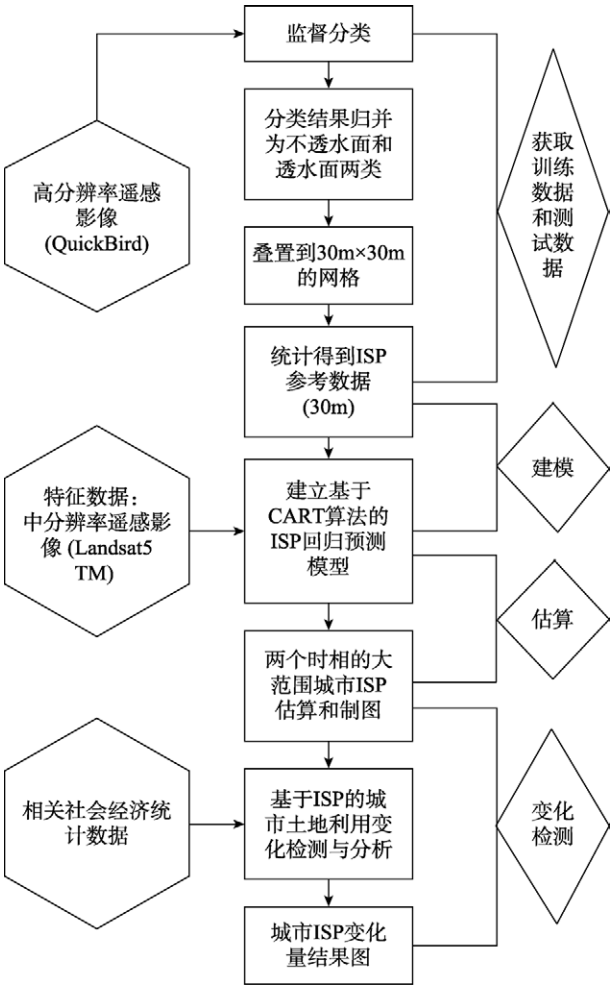

图 1 ISP 遥感估算与城市土地利用变化检测流程图

物目视判读的参考数据。数据成像质量较好，没有云及其阴影的干扰。为了便于后续处理，对上述影像数据进行了预处理。首先利用泰安市 1 10000 比例尺的地形图，对 QuickBird 影像和两幅 TM 影像进行了精确的几何配准，然后经投影和坐标转换后统一到 UTM/WGS84 投影坐标系下；通过重采样后，最终 TM 影像的空间分辨率为 30m。为便于后续的变化检测分析，对 TM 影像进行了辐射定标处理，将各波段 DN 值转化为光谱反射率(NASA, 2009)。

2.2 ISP 遥感估算方法与土地利用变化检测

2.2.1 训练和测试数据的获取

ISP 训练数据和测试数据的获取是 CART 方法的关键步骤，直接关系到最后预测模型的有效性和结果精度，其主要步骤包括: (1)高分辨率遥感影像分类; (2)不透水面百分比参考数据的统计估算(用于模型建立和精度评价)。

运用最大似然分类算法，对研究区域的 0.6m 分辨率的 QuickBird 全色与多光谱融合影像进行监督

分类，得到分类结果的总体精度为 92.56%，Kappa 系数为 0.9112。提取的城市土地利用/覆盖类型包括不透水面(主要由建筑物、道路和水泥面空地等组成)，草地、树木、农田、裸地、水体和阴影。对这一分类结果，统计落在以每个0.6m分辨单元为中心的50×50 像元大小的滑动窗口内的不透水面像元总数，从而可以得到窗口中心像元处的不透水面百分比估计值，最后将估算结果重采样到 TM 影像的 30m 分辨率像元格网上，得到不透水面百分比参考数据，作为预测模型的目标变量。图 3 给出了 QuickBird 原始影像、分类后统计的 0.6m 分辨率格网上的 ISP 结果和重采样到30m分辨率格网上的ISP统计结果。从图 3 看出，在人工建筑物地区一般具有很高的不透水面百分比，植被覆盖地区则很低，而在两者的结合处或混合区，具有中等偏低的百分比。为了满足城区各种透水面和不透水面地物的样本选取(如不同材质、方向、密度和色彩的建筑物)，在实验区内均匀随机选取了 10000 个样本点，其中 8000 个作为训练样本，余下 2000 个作为测试样本，二者相互独立。

特别需要说明的是，考虑到阴影区的实际地物类型无法确定，被分为阴影的像元未参与 ISP 的统计。另外，如果高分辨率影像的获取时间与中等分辨率影像获取时间不一致，在选取 ISP 估算的训练和测试数据时，地表地物类型不一致的样本将被舍弃，以避免造成预测模型的性能降低。

2.2.2 ISP 预测模型的建立

为建立大范围 ISP 的预测模型，以每个时相的 TM 影像除热红外波段以外的 6 个波段的光谱反射率作为预测模型的独立变量，将从 QuickBird 影像分类统计得到的 30m 分辨率 ISP 参考数据作为目标变量。从上述独立变量和目标变量中独立随机抽取若干个样本作为训练数据，运用 CART 算法对这些样本进行学习，建立对应于该时相最终的 ISP 回归预测模型。其中，每棵分类回归树的结构可以很方便地表示成一系列 if—then 形式的决策规则:

规则 1: [2165 cases, mean 44.8, range 1 to 99, est err 15.9]

if

band03≤59

band04 > 75

then

dep = –105.6 + 1.85 band03 + 1.5 band02 –0.72 band04 + 0.44 band06 –0.43 band12 + 0.65 band08 + 0.06 band09 + 0.03 band11

规则 2: [1498 cases, mean 63.8, range 1 to 100, est err 13.4]

if

band03≤59

band04≤75

then

dep = –63.9 + 3.1 band03 –1.45 band04 + 0.8 band09 + 1.02 band02 + 0.3 band05 –0.53 band07 –0.33 band06 + 0.22 band11 –0.04 band12

规则 3: [1527 cases, mean 71.9, range 1 to 100, est err 14.9]

if

band03 > 59

band04 > 77

then

dep = 57.3 + 2.09 band02 –1.12 band03 –1.02 band04 + 0.56 band01 –0.22 band05 + 0.43 band09 + 0.27 band06 –0.35 band07 + 0.22 band10

规则 …

从树的根节点到每一个叶节点的判决路径对应一条决策规则。通过这些规则建立的预测模型其实质是通过分段的多元线性回归来实现非线性的预测分析。在本文研究中，CART 算法的实现采用了 Rulequest 公司的数据挖掘工具软件 Cubist。

2.2.3 ISP 估算与精度评估

建立 2002 年和 2006 年两个 ISP 预测模型后，将其分别应用于对应时相的 TM 影像进行估算，最终得到覆盖整个实验区范围的两期 ISP 估算结果。在进行估算时需要采用水体掩膜，以减少不必要的计算时间开销，加快运算速度。同时，为了验证 ISP 预测模型的有效性，需要利用独立的测试数据对其估算结果进行精度评估。本文利用从高分辨率遥感影像中估算得到的 ISP 作为模型评估的测试数据，采用统计回归分析中的 3 个常用评价指标来评估 ISP 预测模型的质量，即评估实际 ISP 值和预测 ISP 值

(a) (b)

图 2 泰安城区两个时相的 Landsat5 TM 标准假彩色合成图像(红: TM4，绿: TM3，蓝: TM2)
(a) 2002-05-31; (b) 2006-05-02

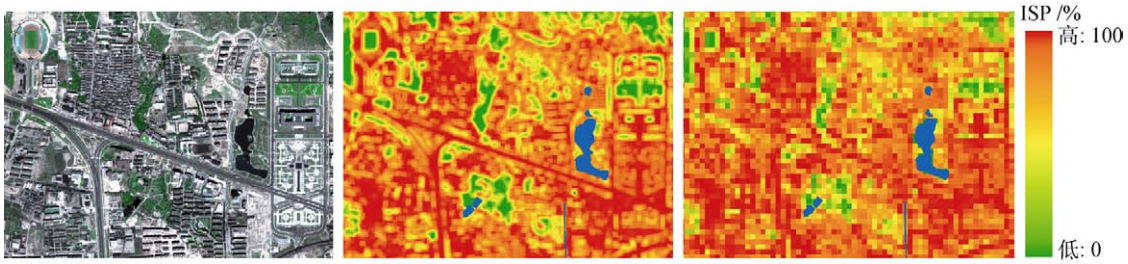

(a) (b) (c)

图 3 ISP 训练/测试数据获取
(a) 0.6m 的 QuickBird 影像; (b) 0.6m 的 ISP 统计结果; (c)重采样到 30m 的 ISP 统计结果。(b)和(c)中蓝色代表水体掩膜

之间的差异大小和线性拟合程度。这 3 个评价指标包括：平均偏差(average error, AE)、相对偏差(relative error, RE)和 Pearson 相关系数(r)，这些指标已在不透水面覆盖度遥感估算的精度评估中得到了广泛的应用(Yang 等，2003a，2003b; Wu & Murray, 2003; Xian & Crane, 2005)。

2.2.4 基于 ISP 的城市土地利用变化检测

利用 2002 年和 2006 年两个时相的 Landsat5 TM 影像进行城区 ISP 估算，利用估算的结果，通过图像差值法，得到 ISP 变化量结果图，在此基础上实现对从 2002 年到 2006 年期间泰安城区的变化情况进行检测和分析。

3 结果与分析

3.1 ISP 估算结果及精度评价

应用建立的 ISP 预测模型，得到 2002 年和 2006 年两期的估算结果如图 4。图中不同的色彩代表了 ISP 值分布的不同区间。从图 4 看出，两个时相的 ISP 估算结果的空间分布格局整体上接近，城区部分大多具有很高的 ISP 值，在 60%以上，老城区的 ISP 值更高，在 80%—100%之间，位于实验区南部郊区(大量农田)和北部的泰山山区(大量树木、草地)则明显低于 40%。其中，植被区域的 ISP 值一般在 30%以下，裸地区域的 ISP 值一般在 40%—50%。实验表明利用中等分辨率的遥感数据能够较好地估算出城市各种地物类型的 ISP 值。

利用前述的 2000 个测试样本，对所建立的 ISP 预测模型的估算性能进行精度评价和比较，评价结果见表 1。同时绘出了测试样本 ISP 预测值和参考值两者的散点图，如图 5。从表 1 结果可以看出，两个时相的 ISP 预测模型性能接近。其中，2006 年的 TM 影像与 QuickBird 影像的获取时间更为接近，因而其对应的预测模型具有稍好的估算性能，相关系数相对于 2002 年高出 0.04，平均误差较 2002 年低了 1.8%。整体上，30m 空间分辨率的 TM 影像存在大量的混合像元，导致只取得了中等偏上的估算结果。图 5 中 ISP 模型预测值和参考值构成的散点图和回归分析结果表明，两个预测模型均在实际 ISP 取值范围的 0—20%区段内存在高估，而在 80%—100%

表 1 泰安实验区两个时相 ISP 预测模型的精度评价

时相	统计指标		
	平均误差(AE)/%	相对误差(RE)	相关系数(r)
2002 年	16.9	0.69	0.67
2006 年	15.1	0.64	0.71

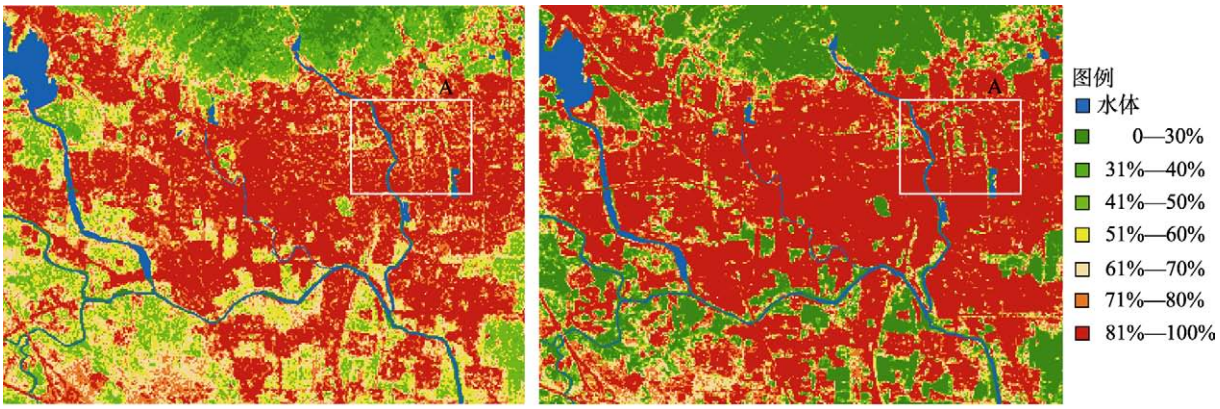

图 4 泰安城区两个时相的 ISP 估算结果

(a) 2002 年; (b) 2006 年

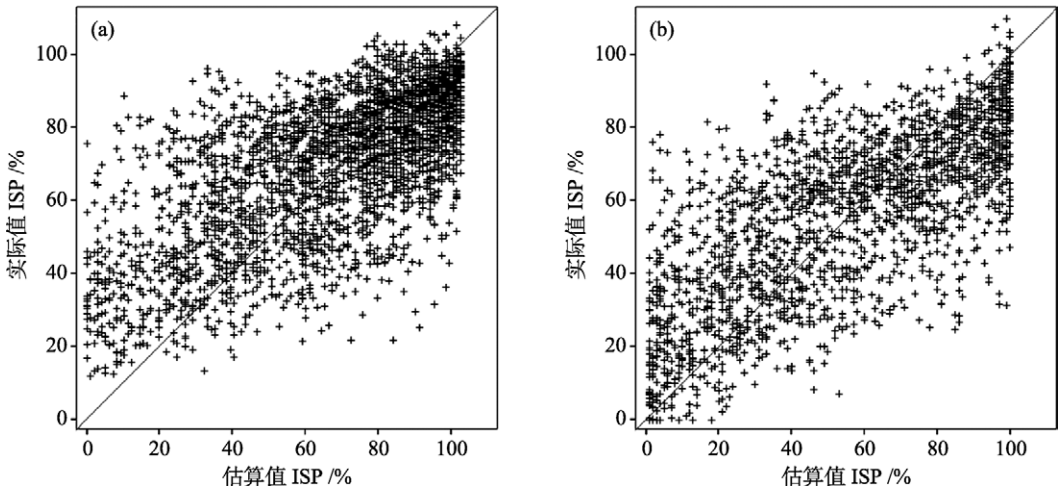

图 5 泰安实验区两个时相的 ISP 估算值和实际值之间散点图

(a) 2002 年; (b) 2006 年

区段上存在低估。

3.2 变化检测实验结果与分析

按照变化检测的基本思想, 将 2002 年与 2006 年的 ISP 估算结果相减, 得到 ISP 变化差异信息。图 6 是实验区内 ISP 增加的区域和变化幅度分布图。从图 4 和图 6 可以看出, 泰安城区从 2002 年到 2006 年期间无论是城区范围还是城区密度都发生了明显的变化。城区范围由 2002 年的老城区和一些城镇扩展到几乎整个实验区, 而且 ISP 增加幅度大于 40%的区域大部分位于城市新建区域。另外, 城区密度也有了很大提高, 主要表现在老城区 ISP 的增加上, 如位于标注 A(图 4)的岱庙附近的老城区, 其 ISP 由 2002 年的 61%—70%提高到 2006 年的 81%—100%。

为便于定量和定性分析, 通过计算得到城区 ISP 增加值超过 30%和减少值超过 40%的区域分布图, 如图 7 所示, 其中图 7(a)中黄色斑块表示 ISP 增加超过 30%的部分, 图 7(b)中绿色斑块表示 ISP 减少超过 40%的部分。结合已有的中、高分辨率遥感影像及该地区地形图, 分析得知图 7 中 A、B、C 区域分别是泰安新建

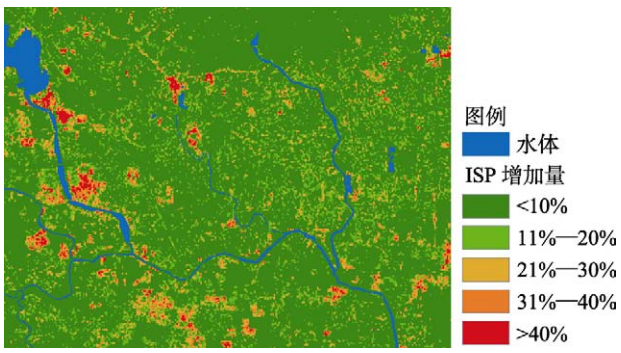

图 6 泰安城区 2002—2006 年 ISP 变化检测结果 (ISP 增加部分)

市政府、大河水库大坝下和泰安市开发区及其周边区域, 这些区域在 2002 年到 2006 年期间进行了大量的城市建设, 造成了这几个区域的 ISP 升高幅度明显超过了 30%; 同期泰安市为打造良好的旅游城市形象, 改善旅游环境, 在国家“十五”期间增加了大量城市绿地, 使得泰山山脚周围(标注 D)和开发区及周边农田(标注 E)区域的 ISP 大幅降低。为了验证 ISP 降低与植被覆盖变化之间的联系, 计算了两个时相 Landsat5 TM 影像的 NDVI 值, 发现标注 D 和 E 对应的绿色区域在 2002 年到 2006 年的 NDVI 值有明显增加, 说明植被覆盖增加是该区域 ISP 减少的主要原因。整体上, 泰安城区的土地利用格局的变化直接表现在城市 ISP 的变化中。

为了分析土地利用变化趋势, 需要采用一定的 ISP 阈值划分城市土地利用类别(Wu & Murray, 2003)。参考已有的研究(Xian & Crane, 2005), 依据不同的 ISP 取值范围将城市土地利用划分为 4 种类型, 定义这 4 种类型的 ISP 经验阈值和主要地物组成见表 2。通过定量统计分析, 得到了泰安实验区内 2002—2006 年之间 4 种土地利用类型面积的变化量, 如表 3。

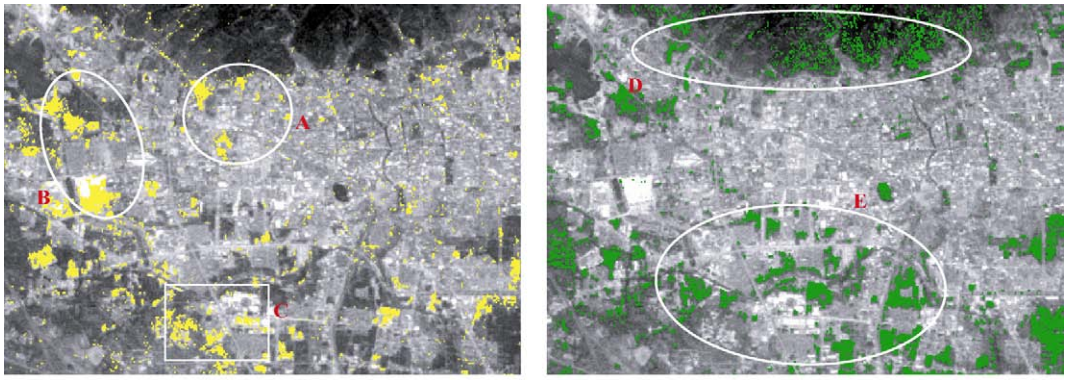

图 7 2002 年至 2006 年间泰安市 ISP 变化结果图

(a) ISP 增加超过 30%, A 为新建市政府, B 是大河水库大坝下区域, C 是泰安市开发区; (b) ISP 减少超过 40%, D 为泰山山脚周边, E 是开发区及周边农田

表 2 根据 **ISP** 范围划分的 **4** 类城市用地类型

4 类城市土地利用	非建设用地	中低密度城镇用地	中高密度城镇用地	高密度城镇用地
ISP 范围/%	<30	31—50	51—80	81—100
主要地物组成	农业用地和城市绿地等	居民地和少量道路等	道路、老城区和商业用地等	商业用地和工业仓储用地等

表 3 泰安城区 **2002—2006** 年 **4** 类土地利用类型变化量 /km^2

土地利用类型	2002 年	2006 年	变化量
非建设用地	5.4774	17.7111	12.2337
中低密度城镇用地	11.7900	7.2720	−4.5180
中高密度城镇用地	36.1089	17.4969	−18.6120
高密度城镇用地	35.1531	46.0494	10.8963
总面积	88.5294		0

根据上述图表中的估算和统计结果, 综合分析后得出从 2002—2006 年, 泰安实验区内的土地利用变化呈现出以下特征:

(1) 城市建设用地内部改造十分明显, 城区密度提高显著, 呈现出中低、中高密度城镇用地逐渐向高密度城镇用地转变的趋势。从 2002—2006 年期间, 实验区内中低、中高密度城镇用地大幅减少, 而高密度城镇用地面积增加了约 10.8963km^2。

(2) 城市绿化建设成绩显著, ISP<30%的非建设用地大量增加, 从 2002—2006 年, 实验区内的非建设用地面积由约 5.4774km^2 增加到约 17.7111km^2, 增加了约 223%。新增加的非建设用地绝大部分是城市绿地。

4 结论与讨论

本文主要研究了利用多时相遥感数据 ISP 估算结果进行城市变化检测的问题, 以泰安作为实验区验证了基于 ISP 的城市土地利用变化检测方法的应用潜力。同传统的变化检测方法相比, 基于 ISP 的变化检测方法综合利用了中、高分辨率遥感数据的优势, 为城市土地利用变化信息的提取和分析提供

了一种新的思路，可以作为现有变化检测方法的有益补充。此外，基于 ISP 的变化检测方法不仅能够提供有关城市土地利用空间格局和密度变化的丰富信息，而且可以灵活地量化定义和解释城市用地变化状况，反映土地利用类型转换趋势的潜在信息。

然而，基于 ISP 的变化检测方法也存在一些不足之处。由于每个时相的 ISP 估算结果均存在 10%—20%的误差，导致在两时相 ISP 差异图中，较小的增长幅度难以有效地反映研究区内实际的地物变化。另外, ISP 变化检测结果的精度也受到以下几个因素的影响：多源(多时相)遥感影像的配准误差和定标误差；ISP 训练数据获取的不确定性和误差，比如高分辨率影像中对阴影的处理，中、高分辨率训练样本的一致性等。随着遥感技术在图像配准、定标和解译能力方面的提高，这些局限性可望得到一定缓解。

REFERENCES

Arnold C L and Gibbons C J. 1996. Impervious surface coverage: the emergence of a key urban environmental indicator. *Journal of the American Planning Association*, **62**(2): 243—258

Brabec E, Schulte S and Richards P L. 2002. Impervious surfaces and water quality: a review of current literature and its implications for watershed planning. *Journal of Planning Literature*, **16**(4): 499—514

Bruzzone L and Serpico S B. 1997. An iterative technique for the detection of land-cover transitions in multitemporal remote-sensing images. *IEEE Transactions on Geoscience and Remote Sensing*, **35**(4): 858—867

Chen S P. 2000. Urbanization and Urban Geographical Information System. Beijing: Science Press

Coppin P, Jonckheere I, Nackaerts K, Muys B and Lambin E. 2004. Digital change detection methods in ecosystem monitoring: a review. *International Journal of Remote Sensing*, **25**(9): 1565—1596

Jia Y H. 2003. Digital Image Processing. Wuhan: Wuhan University Press

Li Q, Li L and Zhao X. 2005. Urban change detection using Landsat TM imagery. *Geomatics and Information Science of Wuhan University*, **30**(4): 351—354

Liu Z, Gong P and Shi P J, Sasagawa T, He C Y. 2005. Study on change detection automatically based on similarity calibration. *Journal of Remote Sensing*, **9**(5): 537—543

Lu D, Mausel P, Brondízio E and Moran E. 2004. Change detection techniques. *International Journal of Remote Sensing*, **25**(12): 2365—2407

Mas J F. 1999. Monitoring land-cover changes: a comparison of change detection techniques. *International Journal of Remote Sensing*, **20**(1): 139—152

NASA. 2009. Chapter 11-Data product. Landsat 7 science data users handbook. http://landsathandbook.gsfc.nasa.gov/handbook/ handbook_htmls/chapter11/chapter11.html#section11.3[2007-07-12]

Radke R J, Andra S, Al-Kofahi O and Roysam B. 2005. Image change detection algorithms: a systematic survey. *IEEE Transactions on Image Processing*, **14**(3): 294—307

Singh A. 1989. Digital change detection techniques using remotely-sensed data. *International Journal of Remote Sensing*, **10**(6): 989—1003

Wu C and Murray A T. 2003. Estimating impervious surface distribution by spectral mixture analysis. *Remote Sensing of Environment*, **84**(4): 493—505

Xian G and Crane M. 2005. Assessments of urban growth in the Tampa Bay watershed using remote sensing data. *Remote Sensing of Environment*, **97**(2): 203—215

Yang L M, Huang C Q, Homer C G, Wylie B K and Coan M J. 2003. An approach for mapping large-area impervious surfaces-synergistic use of Landsat-7 ETM+ and high spatial resolution imagery. *Canadian Journal of Remote Sensing*, **29**(2): 230—240

Yang L M, Xian G, Klaver J M and Deal B. 2003. Urban land-cover change detection through sub-pixel imperviousness mapping using remotely sensed data. *Photogrammetric Engineering and Remote Sensing*, **69**(9): 1003—1010

附中文参考文献

陈述彭. 2000. 城市化与城市地理信息系统. 北京: 科学出版社

贾永红. 2003. 数字图像处理. 武汉: 武汉大学出版社

李全, 李霖, 赵曦. 2005. 基于 Landsat TM 影像的城市变化检测研究. 武汉大学学报·信息科学版, **30**(4): 351—354

刘臻, 宫鹏, 史培军, Sasagawa T, 何春阳. 2005. 基于相似度验证的自动变化探测研究. 遥感学报, **9**(5): 537—543